Supplementary Materials for

Nitrogen fixation mechanisms and distribution patterns of UCYN-A in the global ocean

Subhendu Chakraborty[1,*], Jonathan P. Zehr[2], Ondřej Prášil[3], Wing Kwan Esther Mak[2], Agostino Merico[1,4]

[1]*Systems Ecology Group, Leibniz Centre for Tropical Marine Research (ZMT); 28359 Bremen, Germany*

[2]*Oceans Sciences Department, University of California at Santa Cruz, CA, United States*

[3]*Institute of Microbiology, The Czech Academy of Sciences, Třeboň, Czech Republic*

[4]*Faculty of Biology and Chemistry (FB2), University of Bremen, 28359 Bremen, Germany*

*Corresponding author. Email: subhendu.chakraborty@leibniz-zmt.de

The PDF file includes:

Contents

Supplementary Text

Supplementary Text 1. Model parameterization

Parameters originate from literature sources and were converted to appropriate units as needed.

UCYN-A nitroplast and haptophyte cell sizes and carbon content

Seawater samples from the North Pacific Ocean revealed that UCYN-A nitroplasts, with characteristic sizes between 0.31 to 0.92 μm in diameter, were predominantly associated with haptophyte cells ranging from 0.99 to 1.76 μm in diameter[1]. For our model, we chose diameters, $d_S = 0.6$ μm and $d_H = 1.4$ μm for nitroplasts and the haptophyte, respectively, ensuring that the ratio between the two matches the empirically observed value of 2.33 [2]. With this consideration, we have specifically investigated the dynamics of the clade UCYN-A1.

We choose a thickness of the cell wall (L_{w}) of 10 nm [3], which is same for both cells. Furthermore, by applying a ratio of 29:1 for the radius of cellular cytoplasm (r_C) and plasma membrane (L_{m})[4] and assuming the radius of cells (r) as $r = r_C + L_{\mathrm{m}} + L_{\mathrm{w}}$, we calculated both r_C and L_{m}. These parameters are useful in calculating the reduction in diffusivity of oxygen in the plasma membrane compared to water.

We have obtained the cellular carbon content by using the conversion factor between cellular carbon (C pg) and cell volume (V μm^3) [5] as

$$\log(\mathrm{C}) = -0.363 + 0.863 \times \log V. \qquad (35)$$

Parameters related to photosynthesis and nutrient uptake rates

The values of the parameters related to maximum photosynthetic rate ($J^H_{L,\max}$) of the haptophyte were calibrated using log-transformed empirical data[6] for maximum photosynthetic rate of phytoplankton and the fit of the equation with data is shown in Fig. 2a in the main text. Parameters, a_L and b_L, corresponding to the light affinity (α_L) are calibrated by comparing with empirical data[7] and the fit is shown in Fig. 2b in the main text.

The data for maximum phosphate uptake rate ($J_{P,\max}$) and affinity for phosphate (α_P) for the haptophyte are taken from Marañón et al.[6] and the fits are shown in Fig. 2d,e. Regarding nutrient uptake rates, the data for maximum iron uptake rate ($J_{Fe,\max}$) and affinity for iron (α_{Fe}) are, respectively, taken from Lis et al.[8] and Lory et al.[9], and the fits are shown in Fig. 2g,h.

Previous measurements document a transfer of about 9 – 23 % of fixed C from the haptophyte to UCYN-A1[1,10]. Although, in our present study, the haptophyte cell determines the transfer of C from the haptophyte to nitroplast to maximize its growth rate, we assume that the haptophyte transfers a similar constant amount, 15 % ($\sigma = 0.15$), of Fe and P to the nitroplast.

Parameters related to N_2 fixation rate

For the UCYN-A1 clade, Turk-Kubo et al.[11] measured single cell N_2 fixation rate of 30.5 fmol cell^{-1} d^{-1} with an average of 6.6±8.8 fmol cell^{-1} d^{-1} in Southern California Current System.

The average cell specific N_2 fixation rate for UCYN-A1 from tropical North Atlantic was measured as 12 fmol cell^{-1} d^{-1} [12]. In the present study, we consider the maximum N_2 fixation rate of $M_{N_2} = 20$ fmol cell^{-1} d^{-1} while our cells adjust the actual amount of fixed N_2 based on their requirements which are mainly determined by the surrounding environment.

Cellular ratios of carbon to other nutrients and oxygen

Samples from tropical North Atlantic Ocean show similar C:N ratio of 6.3 mol C (mol N)$^{-1}$ for both the nitroplast and the haptophyte[12]. Accordingly, we have chosen $\rho_{CN} = 6.3$ fmol C (fmol N)$^{-1}$.

Using high-frequency in situ observations of oxygen and carbon concentrations from the North Pacific Ocean, Freitas et al.[13] found a photosynthetic quotient of 0.7 mol C (mol O_2)$^{-1}$ and respiratory quotient of 1 mol C (mol O_2)$^{-1}$. For our purpose, we have used the same values, ρ_{CO}^{P} = 0.7 mol C (mol O_2)$^{-1}$ and ρ_{CO}^{R} = 1 mol C (mol O_2)$^{-1}$, but converted these units to fmol C (µmol O_2)$^{-1}$.

The C:Fe ratio (ρ_{CFe}) of B. bigelowii/UCYN-A is taken similar to the C:Fe ratio of another N_2 fixing organism *Crocosphaera* spp. (0.083 mol C (µmol Fe)$^{-1}$) measured during a laboratory experiment[14]. However, for our purpose, we converted the unit to fmol C (nmol Fe)$^{-1}$.

Unialgal batch cultures of *Trichodesmium erythraeum*, strain IMS101, show C:P ratio (mol C (mol P)$^{-1}$) in the range 209 ± 19.0 to 234 ± 132, whereas *Crocosphaera watsonii*, strain WH8501, show values within 183 ± 19.6 and 260 ± 43.2 [15]. In our model, we used ρ_{CP} = 200 mol C (mol P)$^{-1}$, but changed the unit to fmol C (µmol P)$^{-1}$.

Note that, we assume similar cellular C:N, C:O_2, C:Fe, and C:P ratios for both the haptophyte and nitroplast.

Respiratory costs

The cost of basal maintenance was considered as 0.04 d^{-1} in a previous paper dealing with plankton cells [16]. However, since the nitroplast pays extra cost of maintaining apparatus for N_2 fixation whereas the haptophyte cell needs to maintain cost its symbiont, we have considered an increased basal maintenance cost of R_0 =0.1 d^{-1}. The cost of photosynthesis by the haptophyte is chosen as R_C^H = 0.1 fmol C (fmol C)$^{-1}$, similar to the cost of nitrate uptake provided in [17]. The uptake costs of iron and phosphate are also assumed similar to the cost of photosynthesis, i.e., $R_{\mathrm{Fe}} = R_P = R_C^H$. However, for our purpose, we have changed the units of R_{Fe} and R_P to fmol C (nmol Fe)$^{-1}$ and fmol C (µmol P)$^{-1}$, respectively.

Regarding the direct respiratory cost of N_2 fixation, 2.04 moles carbohydrate is needed to produce one mole of NH_3 [18], which yields R_{N_2} = 2.08 fmol C fmol N^{-1}. The indirect cost of N_2 fixation in terms of oxygen removal from the cell (J_{R,O_2}^{S}) can be obtained by converting the diffusive flux of oxygen in the cell into carbon equivalents (Eq. (3)).

Parameters related to diffusion

UCYN-A nitroplast genome contains genes encoding hopanoid membrane lipids, which are known to restrict oxygen diffusion in the cell through cell membrane layers[19]. However, direct measurements of diffusivity of oxygen through cell membrane layers nitroplast are not available. Previously, Inomura et al. [20] calibrated values (lower than 10^{-3}) of the relative diffusivity of oxygen through the cell membrane of *Trichodesmium* compared to water. Here, we use the same value to account for the reduction oxygen diffusivity through the cell membrane of nitroplast compared to water as $\varepsilon_m^S = 10^{-3}$.

Parameters related to $Q_{10,L}$ values

We chose $a_1 = 0.2$, $a_2 = 6$, $a_3 = 4$, and $a_4 = 2.4$ to match the variations in $Q_{10,L}$ with the empirical data [21,22] and the comparison is shown in Fig. S1.

Supplementary Text 2. Sensitivity analysis

The sensitivity of some of the model components are examined by varying several important parameters by ±25% (Fig. S2) from their default values (Table S1). Specifically, we examine the sensitivity of the parameters related to the diameter of cells (d_S, d_H), parameter determining maximum photosynthetic rate (p_a), respiratory costs (R_0, R_{L}, R_{N_2}), cellular C:N (ρ_{CN}), and Q_{10} values ($Q_{10,R}$, $Q_{10,U}$). We define the sensitivity index (I) as $I = (\bar{X} - X) \times 100/X$, where X is the value of the variable with reference parameters mentioned in Table S1 and $\bar{X}$ is the value of the same variable obtained when the parameter is varied by ±25%. This measure gives the relative change of the variable.

We find that the parameters related to maximum photosynthetic rate and cell sizes influence the system dynamics most.

Supplementary Text 3. General simulation setup

Water column simulation

For the calculation of N_2 fixation in the vertical water column, we chose the variations of the abiotic factors (light, temperature, oxygen, iron, and phosphate) in the vertical water column from the centre of a cyclonic eddy and an anticyclonic eddy near Station ALOHA in the North Pacific Subtropical Gyre [23–25]. The data for light and temperature are taken from Gradoville et al. [23], the oxygen concentrations are taken from World Ocean Atlas [25], and the data for , iron and phosphate are taken from Dugenne et al. [24]. We assume the light attenuation rate (K_Z) as 0.04 m^{-1} (Letelier et al. 2004). For comparing our calculated N_2 fixation rates, we used measured N_2 fixation rates at different depths from Gradoville et al. [23].

Global simulation

For the global simulation, the model is run in the global ocean at every 5° × 5° grid point using vertical fields of annual mean light intensity, temperature, oxygen, iron, and phosphate concentration data as forcing. The data for light intensity are considered as the annual mean absorbed solar radiation taken from Hartmann[26]. The light intensity data was initially converted from W m^{-2} to µmol m^{-2} s^{-1} [27] and then converted from solar radiation to PAR multiplying by 0.48 [28]. Temperature, oxygen, and phosphate concentrations are taken from World Ocean Atlas 2018[25,29,30]. The iron data is taken from Osafuna et al.[31].

The model is constructed in such a way that nitroplast will never be limited by iron or phosphorous. If any of these nutrients is low, the haptophyte will reduce its carbon supply to adjust with nitroplast's requirement and maximize its own growth. However, nutrient limitation can occur in the haptophyte cell. Therefore, to investigate different scenarios of nutrient limitation on the symbiosis, we look at nutrient limitation on the haptophyte cell.

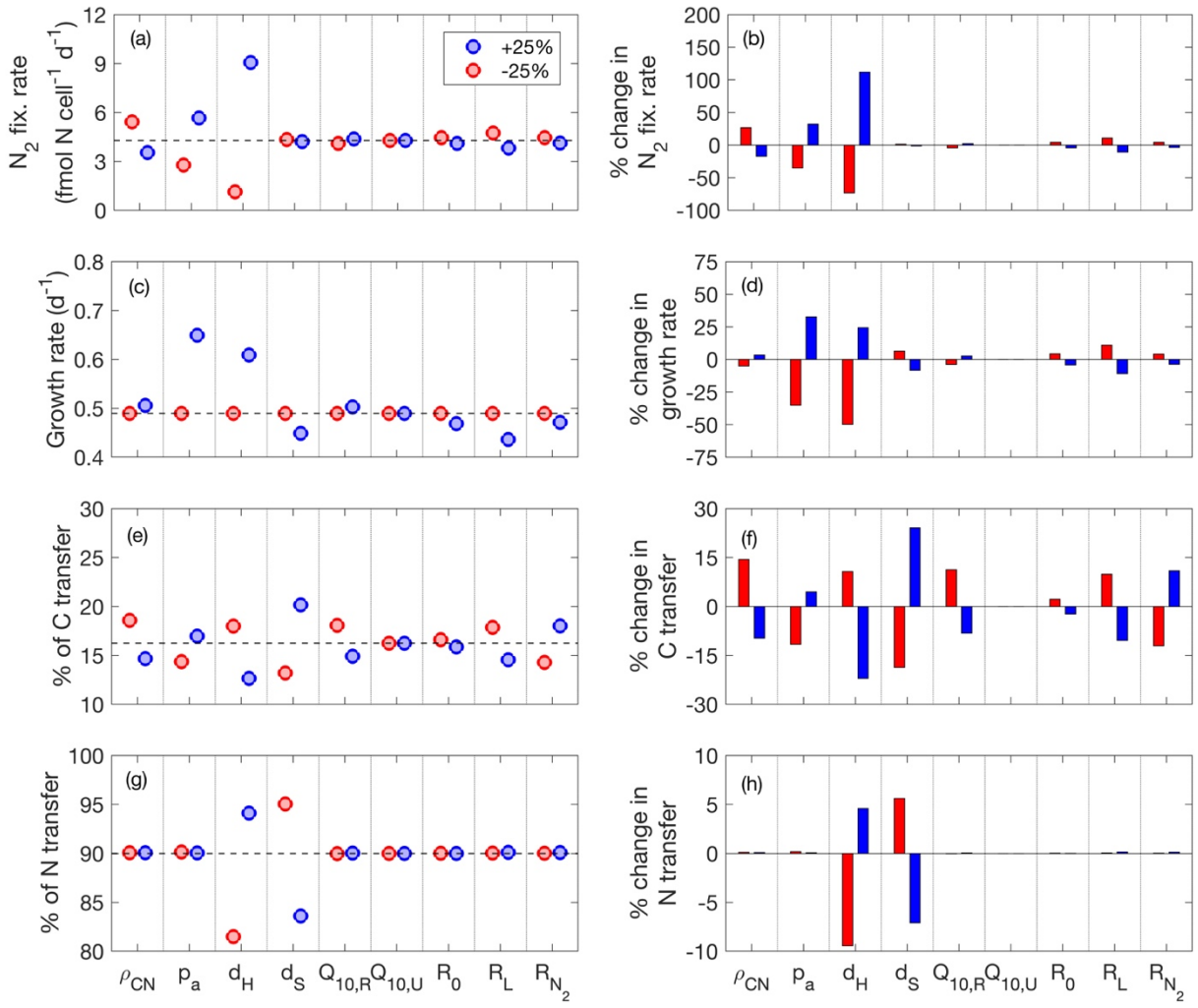

Fig. S1. Sensitivity of some model components with respect to variations in parameters. The variations in (a, b) N_2 fixation rate, (c, d) growth rate, (e, f) % of carbon transfer from the haptophyte to UCYN-A nitroplast, and (g, h) % of nitrogen transfer from the nitroplast to the haptophyte are plotted by varying parameters by +25% (small blue circles) and -25% (small red circles) from their base values. The values of the model components at the base values are indicated by the horizontal lines. First column shows the deviations of components in actual values whereas the second column represents the same but in percentages. We investigate the sensitivity for the parameters (1) C:N value of cells (ρ_{CN}), (2) parameter determining maximum haptophyte photosynthetic rate (p_a), (3) diameter of haptophyte cell (d_H), (4) diameter of nitroplast (d_S), (5) Q_{10} value for respiration ($Q_{10,R}$), (6) Q_{10} value for nutrient uptake ($Q_{10,U}$), (7) basal respiration rate (R_0), (8) respiratory cost of photosynthesis (R_C), (9) respiratory cost of N_2 fixation (R_{N_2}).

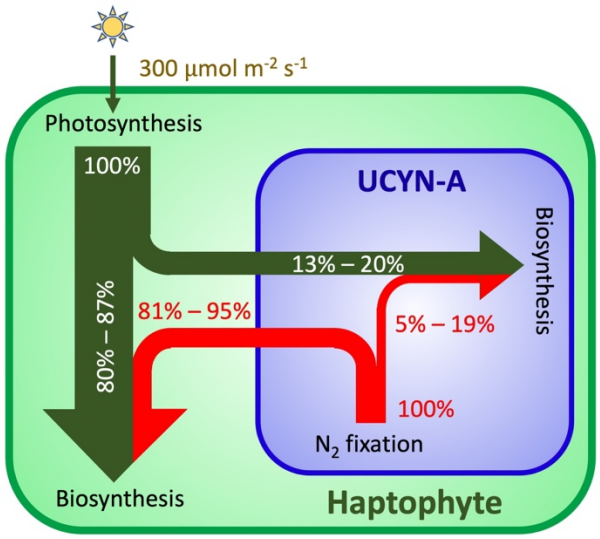

Fig. S2. Conceptual representation of optimal allocation of resources between the two partners obtained from the sensitivity analysis. The haptophyte (green box) transfers 15 – 24 % of the photosynthetically derived carbon to the UCYN-A nitroplast and keeps the other portion for its growth. The nitroplast (blue box) transfers 82 – 95 % of the fixed nitrogen to the haptophyte and uses only 5 – 18% for growth. These fluxes are estimated using sensitivity analysis of our model parameters with a light intensity fixed at 300 µmol m^{-2} s^{-1}.

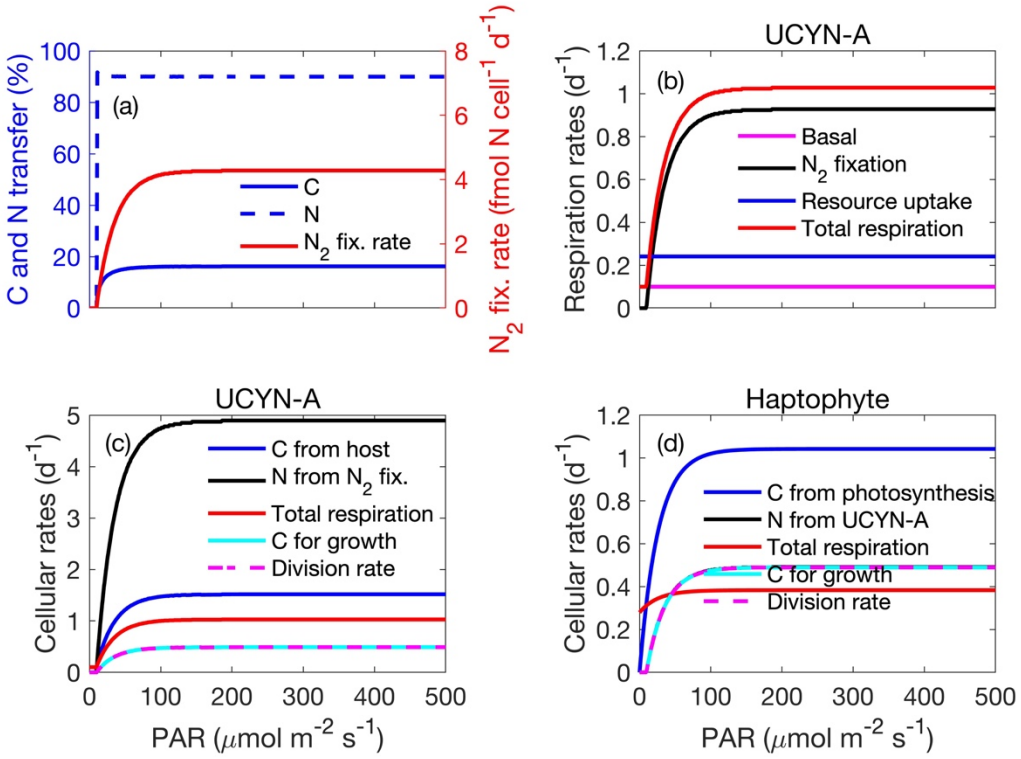

Fig. S3. Cellular rates at different light intensities. (a) % of carbon transfer from the haptophyte to the UCYN-A nitroplast (solid blue), % of nitrogen transfer from the nitroplast to the haptophyte (dashed blue), and the N_2 fixation rate of nitroplast (red). (b) Respiration rates. (c) Cellular rates determining growth in UCYN-A nitroplast. (d) Cellular rates determining growth in the haptophyte.

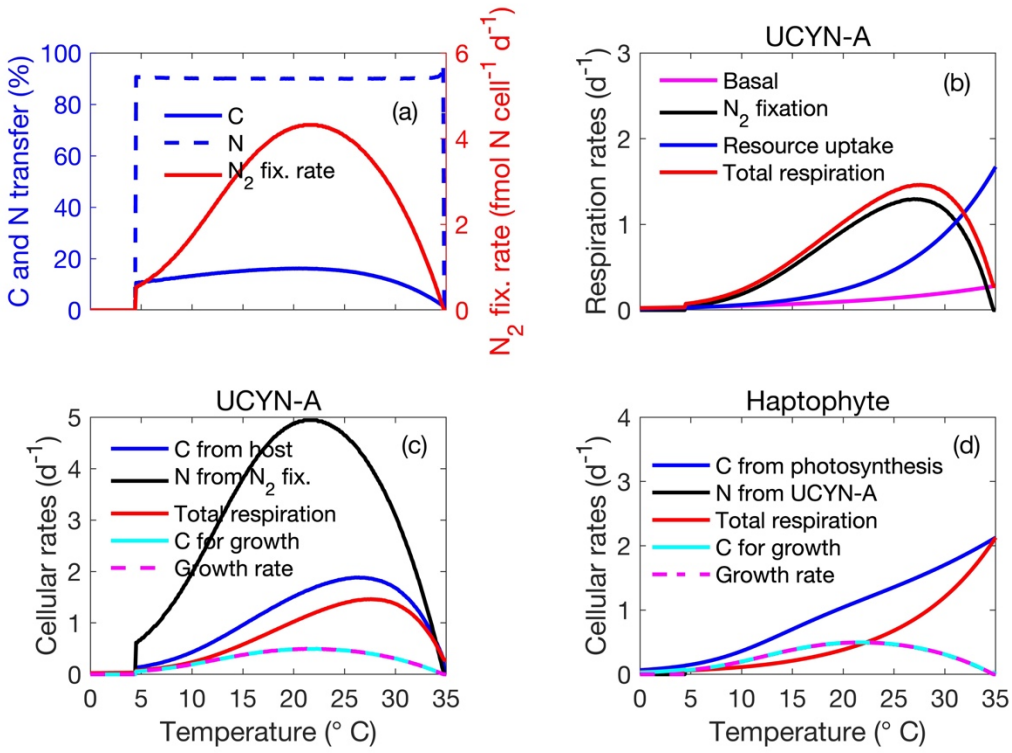

Fig. S4. Cellular rates at different temperatures. (a) % of carbon transfer from the haptophyte to the UCYN-A nitroplast (solid blue), % of nitrogen transfer from the nitroplast to the haptophyte (dashed blue), and the N_2 fixation rate of nitroplast (red). (b) Respiration rates. (c) Cellular rates determining growth in nitroplast. (d) Cellular rates determining growth in the haptophyte.

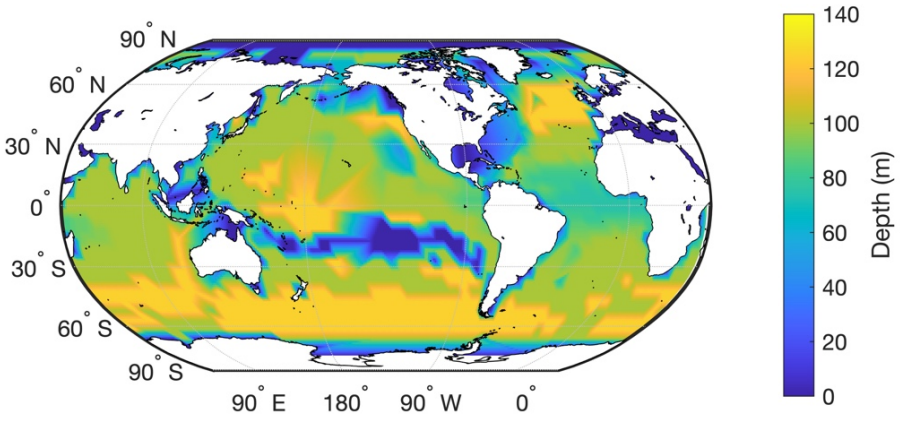

Fig. S5. Global distribution of maximum depth of B. bigelowii/UCYN-A N_2 fixation.

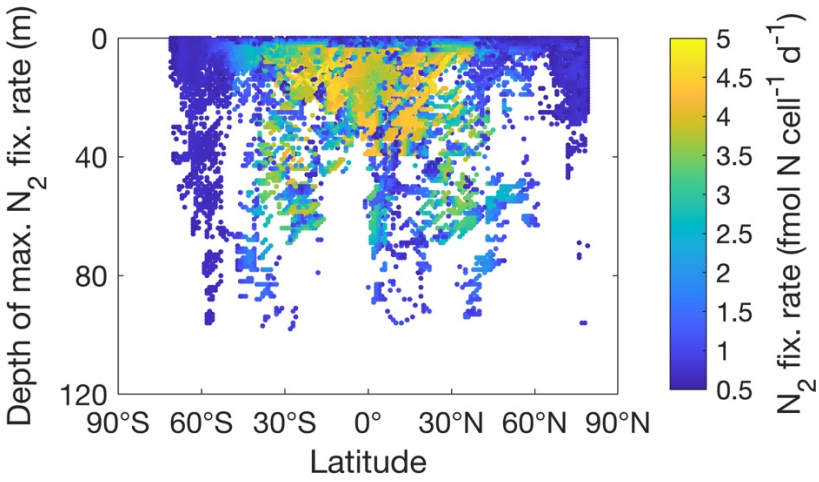

Fig. S6. Latitudinal variation in the depth of maximum B. bigelowii/UCYN-A N_2 fixation in the water column. Many points at the same latitude are from different longitudes.

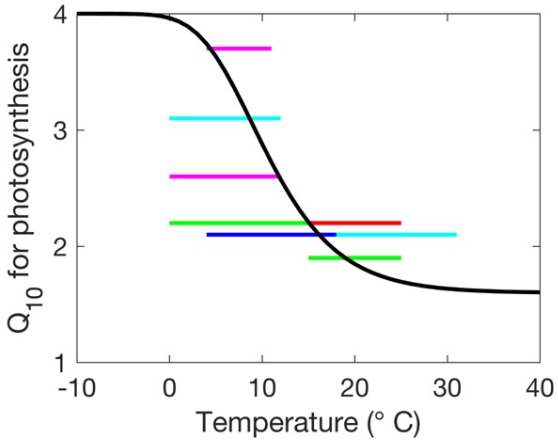

Fig. S7. Variations in Q_{10} values for photosynthesis ($Q_{10,L}$) with temperature. Black line represents the estimated variations in $Q_{10,L}$ values whereas color lines represent empirically measured Q_{10} values for photosynthesis of phytoplankton [21,22] with their ranges of temperature for measurements.

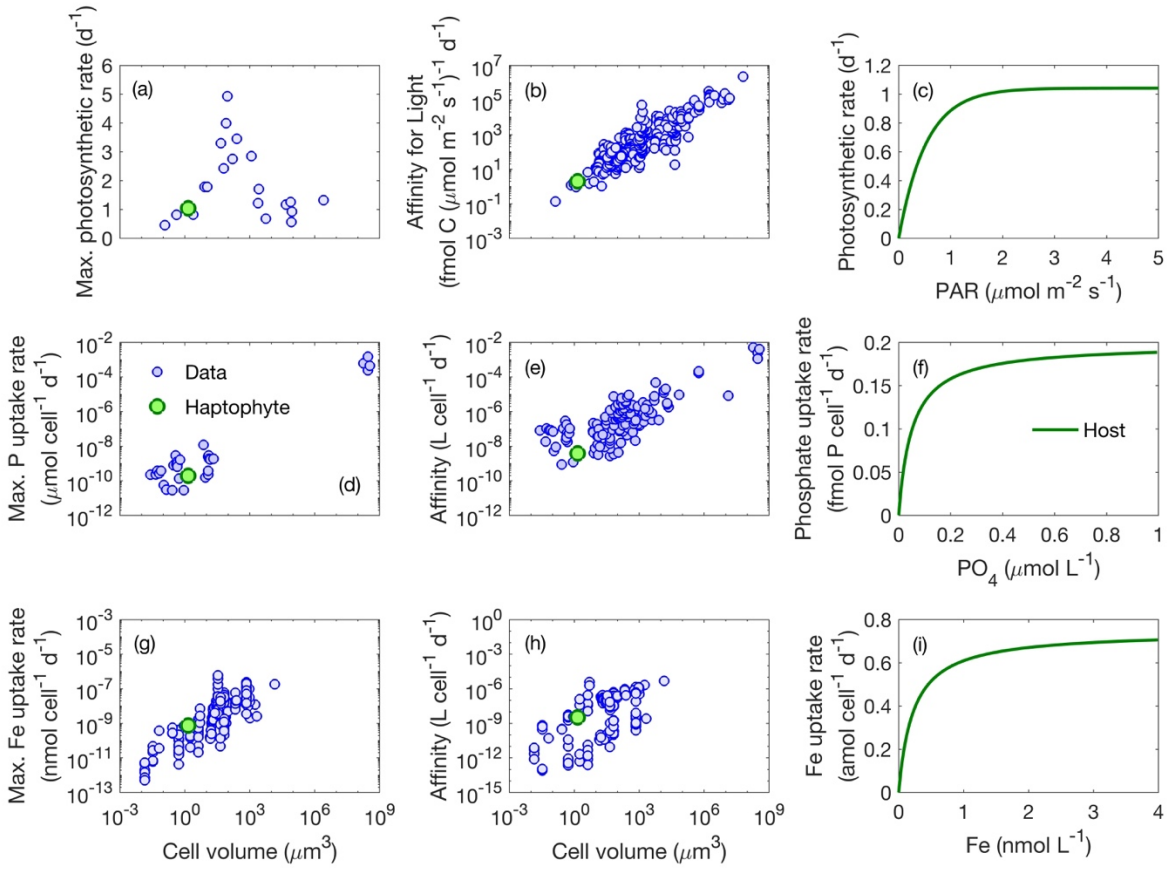

Fig. S8. Calibration of the rate of photosynthesis and phosphate and iron uptake for UCYN-A nitroplast and the haptophyte. Small blue circles represent the data points from different sources and green circles represent our chosen parameter values for the haptophyte. (a) Maximum photosynthetic rate [6]. (b) Affinity for light [7]. (c) Photosynthetic rate of the haptophyte at different light intensities. (d) Maximum phosphate uptake rate [32]. (e) Affinity for phosphate [32,33]. (f) Phosphate uptake rates of the haptophyte at different phosphate concentrations. (g) Maximum iron uptake rate [8]. (h) Affinity for iron [9]. (i) Iron uptake rates of the haptophyte (green) at different iron concentrations.

Table S1. Table containing the parameter values.

Symbol	Description	Value	Unit	Source
d_S	Diameter of nitroplast	0.6	µm	[1]
d_H	Diameter of haptophyte cell	1.4	µm	[1]
r_S	Radius of nitroplast	$d_S/2$	µm	–
r_H	Radius of haptophyte cell	$d_H/2$	µm	–
V_S	Volume of nitroplast	$4/3\pi {r_S}^3$	µm^3	–
V_H	Volume of haptophyte cell	$4/3\pi {r_H}^3$	µm^3	–
C_S	Carbon content in nitroplast	6.8	fmol cell^{-1}	Eq. (35)
C_H	Carbon content in haptophyte	49.4	fmol cell^{-1}	Eq. (35)
p_a	Parameter related to max. photosynthetic rate	3.08		[34]
p_b	Parameter related to max. photosynthetic rate	5.0		[34]
p_c	Parameter related to max. photosynthetic rate	-3.8		[34]
a_L	Parameter related to light affinity	5.0		Calibrated
b_L	Parameter related to light affinity	2.0		Calibrated
$a_{U_{Fe}}$	Multiplicative constant for max. Fe uptake	6×10^{-10}	nmol Fe cell^{-1} d^{-1}	Calibrated
$b_{U_{Fe}}$	Exponent describing size dependence for max. Fe uptake	0.6	–	Calibrated
$a_{\alpha_{Fe}}$	Multiplicative constant for Fe affinity	2.5×10^{-9}	L cell^{-1} d^{-1}	Calibrated
$b_{\alpha_{Fe}}$	Exponent describing size dependence for Fe affinity	0.8	–	Calibrated
a_{U_P}	Multiplicative constant for max. PO_4 uptake	1.5×10^{-10}	µmol P cell^{-1} d^{-1}	Calibrated

b_{U_P}	Exponent describing size dependence for max. PO_4 uptake	0.77	–	Calibrated
a_{α_P}	Multiplicative constant for PO_4 affinity	3×10^{-9}	L cell^{-1} d^{-1}	Calibrated
b_{α_P}	Exponent describing size dependence for PO_4 affinity	0.72	–	Calibrated
M_{N_2}	Max. N_2 fixation rate	20	fmol cell^{-1} d^{-1}	[11]
σ	Fraction of nutrients transferred to nitroplast from haptophyte	0.15	–	[1,10]
ρ_{CN}	Cellular molar C:N ratio	6.3	fmol C (fmol N)$^{-1}$	[12]
ρ_{CO}^{P}	Photosynthetic C:O_2 ratio	7×10^{8}	fmol C (μmol O_2)$^{-1}$	[13]
ρ_{CO}^{R}	Respiratory C:O_2 ratio	1×10^{9}	fmol C (μmol O_2)$^{-1}$	[13]
ρ_{CFe}	Cellular molar C:Fe ratio	8.3×10^{10}	fmol C (nmol Fe)$^{-1}$	[14]
ρ_{CP}	Cellular molar C:P ratio	2×10^{11}	fmol C (μmol P)$^{-1}$	[15]
R_0	Basal respiration	0. 1	d^{-1}	[35]
R_C	Cost of photosynthesis by haptophyte	0.08	fmol C (fmol C)$^{-1}$	[35]
R_{Fe}	Cost of Fe uptake	$\rho_{CFe}R_C$	fmol C (nmol Fe)$^{-1}$	–
R_P	Cost of PO_4 uptake	$\rho_{CP}R_C$	fmol C (μmol P)$^{-1}$	–
R_{N_2}	Cost of N_2 fixation	2.08	fmol C (fmol N)$^{-1}$	[18]
D_{O_2}	Diffusion coefficient of O_2 in water	2.12×10^{-5}	cm^2 s^{-1}	[36]
ε_m^S	Diffusion coefficient of nitroplast cell membrane layers relative to water	1×10^{-3}	–	[37]
a_1	Parameter determining $Q_{10,L}$	0.2	–	Calibrated
a_2	Parameter determining $Q_{10,L}$	6	–	Calibrated
a_3	Parameter determining $Q_{10,L}$	4	–	Calibrated
a_4	Parameter determining $Q_{10,L}$	2.4	–	Calibrated
$Q_{10,R}$	Q_{10} value for respiration	2	–	[38]

$Q_{10,U}$	Q_{10} value for maximum nutrient uptake	2.1	–	[39]
$T_{0,L}$	Reference temperature for photosynthesis	20	°C	Assumed
$T_{0,Fe}$	Reference temperature for iron uptake	20	°C	[40]
$T_{0,P}$	Reference temperature for phosphate uptake	20	°C	[40]
T_{0,R_0}	Reference temperature for basal respiration	20	°C	[39]
T_{0,R_L}	Reference temperature for photosynthetic respiration	20	°C	[41]
$T_{0,R_{N_2}}$	Reference temperature for respiration due to N_2 fixation	28	°C	[18]
$T_{0,D_{O_2}}$	Reference temperature for diffusion of O_2	25	°C	[39]

References

1. Thomspon, A. W. *et al.* Unicellular Cyanobacterium Symbiotic with a Single-Celled Eukaryotic Alga. *Science (80-.).* **337**, 1546–1550 (2012).

2. Cornejo-Castillo, F. M., Inomura, K., Zehr, J. P. & Follows, M. J. Metabolic trade-offs constrain the cell size ratio in a nitrogen-fixing symbiosis. *Cell* **In press**, 1–7 (2024).

3. Yoshida, T., Hairston, N. G. & Ellner, S. P. Evolutionary trade-off between defence against grazing and competitive ability in a simple unicellular alga, Chlorella vulgaris. *Proceedings. Biol. Sci.* **271**, 1947–1953 (2004).

4. Oppenheim, J. & L, M. Correlation of ultrastructure in Azotobacter vinelandii with nitrogen source for growth. *J Bacteriol.* **101**, 286–291 (1970).

5. Verity, P. G. *et al.* Relationships between cell volume and the carbon and nitrogen content of marine photosynthetic nanoplankton. *Limnol. Oceanogr.* **37**, 1434–1446 (1992).

6. Marañón, E. *et al.* Unimodal size scaling of phytoplankton growth and the size dependence of nutrient uptake and use. *Ecol. Lett.* **16**, 371–379 (2013).

7. Edwards, K. F., Thomas, M. K., Klausmeier, C. A. & Litchman, E. Light and growth in marine phytoplankton: allometric, taxonomic, and environmental variation. *Limnol. Oceanogr.* **60**, 540–552 (2015).

8. Lis, H., Shaked, Y., Kranzler, C., Keren, N. & Morel, M. M. Iron bioavailability to phytoplankton : an empirical approach. *ISME J.* **9**, 1003–1013 (2015).

9. Lory, C. *et al.* Assessing the contribution of diazotrophs to microbial Fe uptake using a group specific approach in the Western Tropical South Pacific Ocean. *ISME Commun.* **2**, 41 (2022).

10. Krupke, A. *et al.* The effect of nutrients on carbon and nitrogen fixation by the UCYN-A-haptophyte symbiosis. *ISME J.* **9**, 1635–1647 (2015).

11. Turk-Kubo, K. A. *et al.* UCYN-A/haptophyte symbioses dominate N2 fixation in the Southern California Current System. *ISME Commun.* **1**, 1–13 (2021).

12. Martínez-Pérez, C. *et al.* The small unicellular diazotrophic symbiont, UCYN-A, is a key player in the marine nitrogen cycle. *Nat. Microbiol.* **1**, 1–7 (2016).

13. Freitas, F. H. Diel Measurements of Oxygen - and Carbon - Based Ocean Metabolism Across a Trophic Gradient in the North Paci fi c Global Biogeochemical Cycles. (2020) doi:10.1029/2019GB006518.

14. Tuit, C., Waterbury, J. & Ravizza, G. Diel variation of molybdenum and iron in marine diazotrophic cyanobacteria. *Limnol. Oceanogr.* **49**, 978–990 (2004).

15. Knapp, A. N., Dekaezemacker, J., Bonnet, S., Sohm, J. A. & Capone, D. G. Sensitivity of Trichodesmium erythraeum and Crocosphaera watsonii abundance and N2 fixation rates to varying NO3- and PO43- concentrations in batch cultures. *Aquat. Microb. Ecol.* **66**, 223–236 (2012).

16. Chakraborty, S., Nielsen, L. T. & Andersen, K. H. Trophic Strategies of Unicellular Plankton. *Am. Nat.* **189**, E77--E90 (2017).

17. Pahlow, M. & Oschlies, A. Optimal allocation backs droop's cell-quota model. *Mar. Ecol. Prog. Ser.* **473**, 1–5 (2013).

18. Großkopf, T. & LaRoche, J. Direct and indirect costs of dinitrogen fixation in Crocosphaera watsonii WH8501 and possible implications for the nitrogen cycle. *Front. Microbiol.* **3**, 236 (2012).

19. Cornejo-Castillo, F. M. & Zehr, J. P. Hopanoid lipids may facilitate aerobic nitrogen fixation in the ocean. *Proc. Natl. Acad. Sci. U. S. A.* **116**, 18269–18271 (2019).

20. Inomura, K., Wilson, S. T. & Deutsch, C. Mechanistic Model for the Coexistence of Nitrogen Fixation and and Photosynthesis in Marine Trichodesmium. *mSystems* **4**, e00210-19 (2019).

21. Hancke, K. & Glud, R. N. Temperature effects on respiration and photosynthesis in three diatom-dominated benthic communities. *Aquat. Microb. Ecol.* **37**, 265–281 (2004).

22. Robarts, R. D. & Zohary, T. Temperature effects on photosynthetic capacity, respiration, and growth rates of bloom-forming cyanobacteria. *New Zeal. J. Mar. Freshw. Res.* **21**, 391–399 (1987).

23. Gradoville, M. R. *et al.* Light and depth dependency of nitrogen fixation by the non-photosynthetic, symbiotic cyanobacterium UCYN-A. *Environ. Microbiol.* **23**, 4518–4531 (2021).

24. Dugenne, M. *et al.* Nitrogen Fixation in Mesoscale Eddies of the North Pacific Subtropical Gyre: Patterns and Mechanisms. *Global Biogeochem. Cycles* **37**, e2022GB007386 (2023).

25. Garcia, H. E. *et al. World Ocean Atlas 2018, Volume 3: Dissolved Oxygen, Apparent Oxygen Utilization, and Oxygen Saturation*. *NOAA Atlas NESDIS* vol. 83 https://www.nodc.noaa.gov/OC5/woa18/pubwoa18.html (2018).

26. Hartmann, D. L. *Global physical climatology*. (Elsevier Press, 2016).

27. Thomas, C. *et al.* Smart Approaches for Evaluating Photosynthetically Active Radiation at Various Stations Based on MSG Prime Satellite Imagery. *Atmosphere (Basel).* **14**, 1259 (2023).

28. Tsubo, M. & Walker, S. Relationships between photosynthetically active radiation and

clearness index at Bloemfontein, South Africa. *Theor. Appl. Climatol.* **80**, 17–25 (2005).

29. Locarnini, M. *et al.* World Ocean Atlas 2018, Volume 1: Temperature. *NOAA Atlas NESDIS* **81**, 52 (2018).

30. Garcia, H. E. *et al. World Ocean Atlas 2018, Volume 4: Dissolved Inorganic Nutrients (phosphate, nitrate and nitrate+nitrite, silicate)*. *NOAA Atlas NESDIS* vol. 84 https://archimer.ifremer.fr/doc/00651/76336/ (2018).

31. Osafune, S., Masuda, S., Sugiura, N. & Doi, T. Evaluation of the applicability of the Estimated State of the Global Ocean for Climate Research (ESTOC) data set. *Geophys. Res. Lett.* **42**, 4903–4911 (2015).

32. Lomas, M. W., Bonachela, J. A., Levin, S. A. & Martiny, A. C. Impact of ocean phytoplankton diversity on phosphate uptake. (2014) doi:10.1073/pnas.1420760111.

33. Lindemann, C., Fiksen, Ø., Andersen, K. H. & Aksnes, D. L. Scaling Laws in Phytoplankton Nutrient Uptake Affinity. *Front. Mar. Sci.* **3**, 26 (2016).

34. Ward, B. A. & Follows, M. J. Marine mixotrophy increases trophic transfer efficiency, mean organism size, and vertical carbon flux. *Proc. Natl. Acad. Sci. U. S. A.* **113**, 2958–2963 (2016).

35. Chakraborty, S., Nielsen, L. T. & Andersen, K. H. Trophic strategies of unicellular plankton. *Am. Nat.* **189**, (2017).

36. McCabe, M. & Laurent, T. C. edge of the respiration rates of the aortal walls it is possible to calculate transport coefficients for oxygen through the wall of the artery . Again b y such a method the results obtained are considerably lower than the values quoted for oxygen diffusio. *Biochim. Biophys. Acta* **399**, 131–138 (1975).

37. Inomura, K., Bragg, J. & Follows, M. J. A quantitative analysis of the direct and indirect costs of nitrogen fixation: A model based on Azotobacter vinelandii. *ISME J.* **11**, 166–175 (2017).

38. Eppley, R. W. Temperature and phytoplankton growth in the sea. *Fish. Bull.* **70**, 1063–1085 (1972).

39. Raven, J. & Geider, R. Temperature and algal growth. *New Phytol.* **110**, 441–461 (1988).

40. Ward, B. A., Dutkiewicz, S., Jahn, O. & Follows, M. J. A size-structured food-web model for the global ocean. *Limnol. Oceanogr.* **57**, 1877–1891 (2012).

41. Chakraborty, S. *et al.* Quantifying nitrogen fixation by heterotrophic bacteria in sinking marine particles. *Nat. Commun.* **12**, (2021).